Dynamical crossover in the clock model with a conserved order parameter

Sanjay Puri,[1,2] Rajeev Ahluwalia,[1] and Alan J. Bray[2]
[1]*School of Physical Sciences, Jawaharlal Nehru University, New Delhi 110067, India*
[2]*Department of Theoretical Physics, The University of Manchester, Manchester M13 9PL, United Kingdom*
(Received 30 October 1996)

We present comprehensive numerical results for phase ordering dynamics in the clock model with a conserved order parameter. Our study is based on a dynamical model for a coarse-grained complex order parameter. We find that there is a dynamical crossover from vortex-driven growth at early times to interface-driven growth at later times. The crossover time is later for higher values of the ground-state degeneracy of the clock model. [S1063-651X(97)01303-2]

PACS number(s): 64.60.Cn, 05.70.Fh, 64.60,My

I. INTRODUCTION

The problem of phase ordering dynamics has emerged as a paradigm for nonequilibrium statistical mechanics. Interest in this area focuses on the growth of order in a disordered system which has been suddenly quenched to a region of its phase diagram where the equilibrium state is ordered [1]. Such problems have been extensively studied in the context of two-phase mixtures. For example, a ferromagnet is disordered at high temperatures. When this system is quenched below the critical temperature, it tends to be spontaneously magnetized (or ordered) and domains rich in ''up'' or ''down'' spins are formed. These domains correspond to equivalent ground states of the system at the lower temperature. They coarsen with the passage of time and are characterized by a time-dependent length scale $L(t)$. Thus the morphology of the evolving pattern is unchanged in time other than the growth of the characteristic length scale.

The absence of change in the morphology is reflected in the dynamical scaling of the correlation function $G(\vec{r},t)=\int d\vec{R}\,\psi(\vec{R},t)\,\psi(\vec{R}+\vec{r},t)$, where $\psi(\vec{R},t)$ is the order parameter (i.e., spontaneous magnetization) of the system at point $\vec{R}$ at time t. For isotropic phase ordering systems, the correlation function has the simple dynamical scaling form $G(\vec{r},t)=g(r/L(t))$, where $g(x)$ is a time-independent master function [2]. Experimentally, a more interesting quantity is the time-dependent structure factor $S(\vec{k},t)$, which is the Fourier transform of $G(\vec{r},t)$ with wave vector $\vec{k}$. For the structure factor, the dynamical scaling property takes the form $S(\vec{k},t)=L(t)^d\Phi(kL(t))$, where d is the dimensionality; and $\Phi(x)$ is another master scaling function.

As there is no conservation constraint on the order parameter in the ordering of a ferromagnet, this problem is said to be characterized by a nonconserved order parameter (NCOP). A related problem is that of phase separation in binary (AB) mixtures. Homogeneous binary mixtures can be rendered thermodynamically unstable by quenching below the critical temperature. The homogeneous mixture then separates out into A- and B-rich domains, which are also characterized by a time-dependent length scale and an invariant morphology. However, the dynamics of phase separation is described in terms of a conserved order parameter (COP) because of the constraint that total numbers of A and B atoms must be unchanged during the coarsening process.

There have been extensive experimental, numerical, and analytical investigations of phase ordering dynamics in two-phase mixtures with a scalar Ising-type order parameter [1]. In this paper we focus on pure and isotropic systems so we only quote results therefrom. For the NCOP case, it is well established that the asymptotic domain growth law is $L(t)\sim t^{1/2}$, which is referred to as the Lifshitz-Cahn-Allen or LCA law. Furthermore, there is a reasonable analytical understanding of the functional form of the master function $F(x)$ corresponding to the scaled structure factor [3]. For the COP case also, it is well established that the asymptotic domain growth law is $L(t)\sim t^{1/3}$, which is referred to as the Lifshitz-Slyozov or LS growth law. However, to the best of our knowledge, there is still no complete theoretical understanding of the functional form of the structure factor even though there have been a number of detailed studies [4].

There have also been some investigations of phase ordering dynamics in systems with multiply degenerate ground states (e.g., clock and Potts models); and systems with vector order parameters, where the ground state has a continuous symmetry. In the clock and Potts models, the ''spin'' at each site can take any of (say) q equivalent values. These equivalent states can be conveniently pictured as lying evenly spaced on the perimeter of a circle, i.e., the states for a q-state model are $S=2\pi n/q$, where n ranges from 1 to q. The microscopic Hamiltonian for the clock model on a lattice takes the form [5]

$$H=-J\sum_{\langle ij\rangle}\cos(S_i-S_j), \tag{1}$$

where J is an exchange interaction, S_i denotes the state at lattice site i, and $\langle ij\rangle$ denotes a sum over nearest-neighbour pairs. The corresponding Hamiltonian for the Potts model is [5]

$$H=-J\sum_{\langle ij\rangle}\delta_{S_i,S_j}, \tag{2}$$

where $\delta_{i,j}$ is the Kronecker delta. The Hamiltonians in both Eqs. (1) and (2) reduce to the usual Ising model for the case $q=2$. The clock and Potts models have found extensive ap-

plication in the context of adsorption on surfaces, ordering of multicomponent mixtures, branched polymers, soap froths, and the growth of metallic grains [5].

In this paper we focus on phase ordering dynamics in the clock model with a conserved order parameter. Therefore we would like to briefly summarize extant numerical results for systems with multiply degenerate ground states. For the NCOP case, it is numerically well established that asymptotic domain growth in both the clock and Potts models is characterized by the LCA growth law [6,7], regardless of the ground-state degeneracy q. At late times, the structure factor exhibits dynamical scaling, and analytical studies indicate that the functional form of the scaled structure factor is q dependent [8,9].

The q-state clock model is of considerable theoretical interest as it interpolates between the Ising model (where $q=2$) and the continuous-symmetry XY model (where $q=\infty$). Domain growth in the Ising model is driven by the annealing of interfacial defects, whereas the corresponding defects in the XY model are vortices. In the clock model, domain growth occurs via the annihilation of both interfaces and vortices. It is our expectation that phase ordering in the q-state clock model will initially exhibit an XY-like behavior before crossing over to the asymptotic forms discussed above. The physical origin of this crossover can be understood as follows. The typical angle between spins on neighboring sites of the lattice at time t is $\theta(t)\sim 1/L(t)$, where the characteristic domain size $L(t)$ measures the spacing between defects. At early times, $\theta(t)$ is much larger than the clock quantization angle $\theta_q=2\pi/q$. Therefore, at early times, the local spin variable is effectively ''continuous'' and the system behaves like an XY model. The underlying discrete spin structure is felt when $\theta(t)\sim\theta_q$, i.e., $L(t)\sim$ const$\times q$, and this corresponds to a crossover from XY-like behavior to the true asymptotic behavior. Of course, as the domain growth law is $L(t)\sim t^{1/2}$ for both the Ising and XY models [10] in the NCOP case, the domain growth law will not exhibit a crossover. Unfortunately, the quality of numerical data available [6] is not good enough to distinguish whether or not there is such a crossover in the structure factor.

The COP case with multiply degenerate ground states has received far less attention in the literature, partly because of the lack of experimental realizations. The COP clock model with $q=3$ has been studied by Enomoto *et al.* [11], who find an asymptotic domain growth law consistent with $L(t)\sim t^{1/3}$, which is the LS growth law for the Ising case. There have also been some preliminary Monte Carlo (MC) studies of the COP Potts model [12], but these are not conclusive as regards the nature of dynamical scaling and the asymptotic domain growth law.

In this paper we present results from a comprehensive numerical study of phase ordering dynamics in the COP clock model in both two- and three-dimensional space. There are two primary goals of this study. First, unlike in the NCOP case, we expect a dynamical crossover in the domain growth law from $L(t)\sim t^{1/4}$ in $d=2$ or $L(t)\sim(t\ln t)^{1/4}$ in $d=3$ (which characterizes COP domain growth driven by vortices [13–15]) to the asymptotic form $L(t)\sim t^{1/3}$ (i.e., the usual LS growth law). We would like to elucidate the details of this crossover. We have already clarified the physical origins of this crossover in the context of the NCOP clock model. If we ignore the logarithmic correction to the XY growth law in $d=3$, we can incorporate both early- and late-time behaviors into the simple crossover scaling form $L(t)=t^{1/4}F(t^{1/4}/q)$, where $F(0)$ is a constant. To recover the asymptotic LS growth law, we must have $F(x)\sim x^{1/3}$ for large x, so that $L(t)\sim q^{-1/3}t^{1/3}$ for large t. Thus the amplitude of the asymptotic LS growth law decreases with q as $q^{-1/3}$, though there may be some anomalous cases, as we will see later. The second goal of this study is to examine the nature of the dynamical crossover in the scaled structure factor. As we have mentioned earlier, there is still no good theoretical understanding of the functional form of the scaled structure factor for phase separation in binary mixtures, which is characterized by a scalar order parameter. For the COP case with vector order parameter, it is possible that approximations based on Gaussian closure schemes may be more successful [15] though it is somewhat premature to make such a claim. Comprehensive numerical results serve as an important guide to analytical investigations. In this paper we would like to provide detailed numerical results for the dynamical behavior of the structure factor in the phase ordering dynamics of the COP clock model and hope that these may be of relevance to theorists.

This paper is organized as follows. In Sec. II we present our phenomenological model for phase ordering dynamics in the clock model with a conserved order parameter. Sections III and IV present numerical details and results for the two-dimensional (2D) and 3D cases, respectively. Section V ends this paper with a brief summary and discussion.

II. DYNAMICAL MODEL

The starting point for the simulations we report here is a phenomenological dynamical model obtained as the conserved counterpart of the time-dependent Ginzburg-Landau (TDGL) model [11,8], viz.,

$$\frac{\partial\psi(\vec{r},t)}{\partial t}=\nabla^2\left[\frac{\delta H[\psi(\vec{r},t)]}{\delta\psi(\vec{r},t)^*}\right], \tag{3}$$

where $\psi(\vec{r},t)$ is a complex order parameter which characterizes the state of the system at point $\vec{r}$ and time t, and * denotes complex conjugation. The dimensionless free energy for the continuum q-state clock model below the critical temperature [11,8] is

$$H[\psi(\vec{r},t)]=\int d\vec{r}\,[|\vec{\nabla}\psi(\vec{r},t)|^2-|\psi(\vec{r},t)|^2+\frac{1}{2}|\psi(\vec{r},t)|^4 - \frac{\alpha}{q}[\psi(\vec{r},t)^q+\psi(\vec{r},t)^{*q}-2|\psi(\vec{r},t)|^q]], \tag{4}$$

where $\alpha(>0)$ is a parameter. Replacing Eq. (4) in Eq. (3), we get the dynamical equation

$$\frac{\partial\psi(\vec{r},t)}{\partial t}=-\nabla^2\{\psi(\vec{r},t)[1-|\psi(\vec{r},t)|^2]+\alpha\psi(\vec{r},t)^{*(q-1)} - \alpha\psi(\vec{r},t)^{*(q/2-1)}\psi(\vec{r},t)^{q/2}+\nabla^2\psi(\vec{r},t)\}. \tag{5}$$

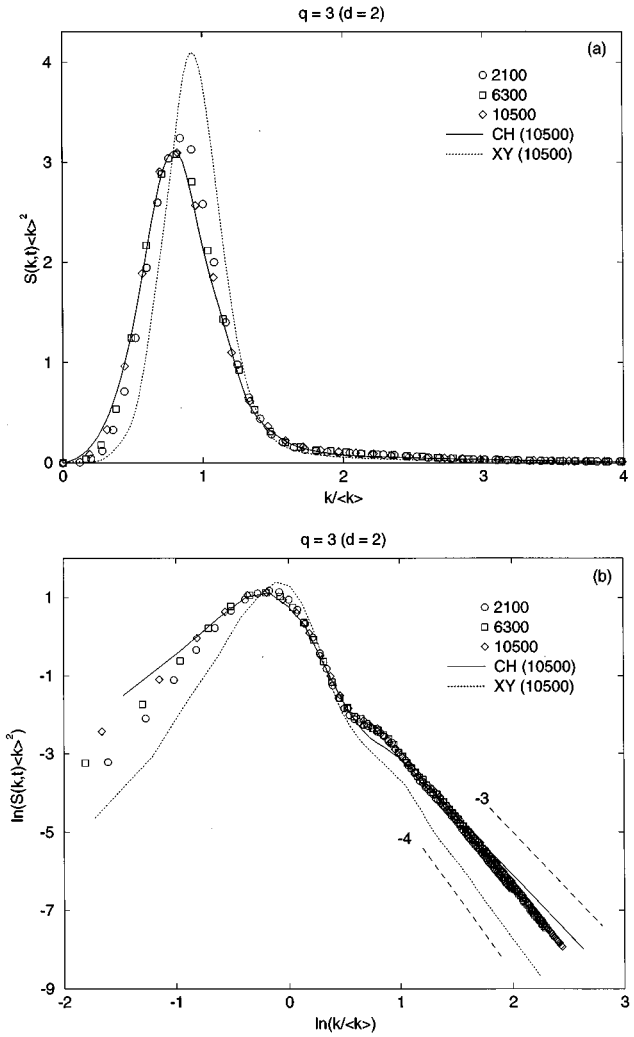

FIG. 1. (a) Data for the scaled structure factor $S(k,t)\langle k\rangle^2$ vs $k/\langle k\rangle$, obtained from a 2D simulation of phase ordering dynamics in the $q=3$ clock model with a conserved order parameter. The structure factor data are obtained on a 256^2 lattice with periodic boundary conditions and are averaged over 80 independent runs. The initial condition for each run consists of small-amplitude random fluctuations about a zero background. The order parameter field is hardened before computing the structure factor. Results presented here are for the spherically averaged structure factor $S(k,t)$. The quantity $\langle k\rangle$ is the first moment of the structure factor and is calculated as described in the text. The structure factor data in this figure correspond to dimensionless times 2100, 6300, and 10 500. For purposes of comparison, we have also superposed data from dimensionless time 10 500, obtained from similar simulations of the CH model (solid line) and the XY model (dashed line). (b) Data from (a), plotted on a log-log scale. The long-dashed lines have slopes -3 and -4, as indicated, and refer to the Porod tail for the CH model and the generalized Porod tail [10] for the XY model, respectively.

The static solutions $\psi^s(\vec{r})$ of Eq. (5) arise from

$$\psi^s(\vec{r})[1-|\psi^s(\vec{r})|^2]+\alpha[\psi^s(\vec{r})^{*(q-1)} - \psi^s(\vec{r})^{*(q/2-1)}\psi^s(\vec{r})^{q/2}]+\nabla^2\psi^s(\vec{r})=0, \quad (6)$$

and the homogeneous fixed points are $\psi_0=e^{iS}$, where $S=2\pi n/q$, with n ranging from 1 to q. These correspond to the q equivalent ground states of the clock model and disordered initial conditions evolve into domains which are rich in one of these states. (Our earlier arguments regarding a dynamical crossover in the clock model were in the context of a lattice model with a hard spin constraint. In the continuum model we use here, the defect core size constitutes a microscopic length scale similar to the lattice spacing. However, if the constraint in the continuum model is reasonably hard [i.e., $\alpha\sim O(1)$], we can expect the previous arguments to apply here also.) The overall conservation constraint imposes the restriction that $\int d\vec{r}\,\psi(\vec{r},t)$ is fixed during the evolution. The limiting cases $q=2$ and $q=\infty$ for Eqs. (3) and (4) correspond to the usual Cahn-Hilliard (CH) and XY models, respectively.

In this paper we numerically simulate Eq. (5) using the simple Euler discretization scheme on a square lattice with periodic boundary conditions. For the numerical scheme to be useful, it must mimic the physics of the continuum equation [16]. Thus the homogeneous solutions of Eq. (5), i.e., $\psi(\vec{r},t)=\psi_0$, should be stable in the discrete scheme also. This imposes a constraint on the discretization mesh sizes, which can be obtained as follows. In Eq. (5), we consider small fluctuations $\phi(\vec{r},t)$ around the homogeneous solution $\psi_0=1$ as $\psi(\vec{r},t)=1+\phi(\vec{r},t)$. (Identical results will arise for fluctuations around any of the other homogeneous solutions.) If we linearize Eq. (5) in $\phi(\vec{r},t)$, we obtain

$$\frac{\partial\phi(\vec{r},t)}{\partial t}=-\nabla^2\left[-\left(1+\frac{\alpha q}{2}\right)\phi(\vec{r},t)-\left(1-\frac{\alpha q}{2}\right)\phi(\vec{r},t)^* + \nabla^2\phi(\vec{r},t)\right]. \quad (7)$$

Writing $\phi(\vec{r},t)=a(\vec{r},t)+ib(\vec{r},t)$, we obtain

$$\frac{\partial a(\vec{r},t)}{\partial t}=-\nabla^2[-2a(\vec{r},t)+\nabla^2 a(\vec{r},t)],$$

$$\frac{\partial b(\vec{r},t)}{\partial t}=-\nabla^2[-\alpha q b(\vec{r},t)+\nabla^2 b(\vec{r},t)]. \quad (8)$$

We can Fourier transform these equations and obtain their discrete equivalents in Fourier space as follows:

$$a(k_D,t+\Delta t)=[1-\Delta t k_D^2(2+k_D^2)]a(k_D,t),$$

$$b(k_D,t+\Delta t)=[1-\Delta t k_D^2(\alpha q+k_D^2)]b(k_D,t). \quad (9)$$

In Eq. (9), the discretization mesh sizes in time and space are Δt and Δx, respectively. Furthermore, the magnitude of the wave vector $k_D^2=(2/\Delta x^2)[d-\Sigma_{i=1}^d\cos(k_i\Delta x)]$. To avoid unphysical subharmonic fluctuations [16], the mesh sizes must satisfy the stronger of the two constraints

$$\frac{\Delta x^4}{2d(2\Delta x^2+4d)}>\Delta t,$$

$$\frac{\Delta x^4}{2d(\alpha q\Delta x^2+4d)}>\Delta t. \quad (10)$$

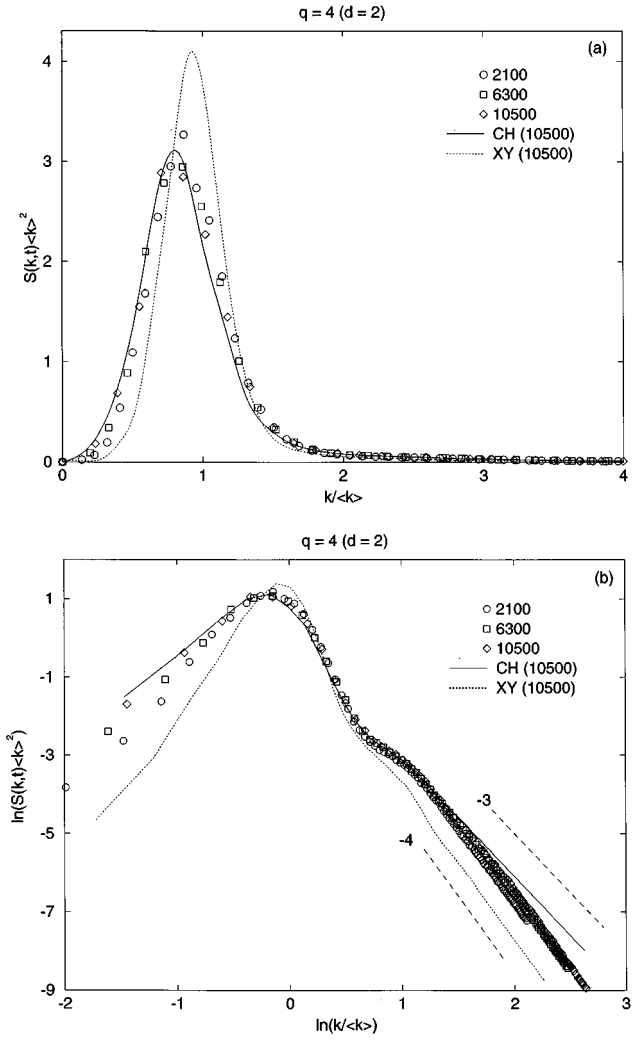

FIG. 2. (a) Analogous to Fig. 1(a), but for $q=4$. (b) Data from (a), plotted on a log-log scale. The long-dashed lines have the same meaning as in Fig. 1(a).

In the CH and XY limits, only the first of these constraints applies.

III. NUMERICAL RESULTS FOR $d=2$

We have simulated an Euler-discretized version of Eq. (5) on a 2D square lattice of size $N\times N$. Periodic boundary conditions were applied in both directions. We fixed the parameter value $\alpha=0.4$ and obtained results for $q=3$, 4, 5, and 7. For purposes of comparison, we also obtained results for the CH ($q=2$) and the XY ($q=\infty$) cases. Our discretization mesh sizes were $\Delta t=0.15$ and $\Delta x=1.7$.

The statistically relevant quantity is the time-dependent structure factor $S(\vec{k},t)=\langle\psi(\vec{k},t)\psi(\vec{k},t)^*\rangle$, which we have defined earlier in the scalar context. All structure factor data presented below are obtained for $N=256$ as an average over 80 independent runs. The initial condition for each run consisted of uniformly distributed random fluctuations about a zero background, mimicking the high-temperature disordered state prior to the quench. On the discrete lattice, the wave vector $\vec{k}$ takes discrete values $\vec{k}=(2\pi/N)(k_x,k_y)$, where k_x and k_y range from $-N/2$ to $N/2-1$. To improve the quality of our data, we spherically averaged $S(\vec{k},t)$ to obtain the scalarized structure factor $S(k,t)$, which we present subsequently. Apart from the structure factor, we are also interested in the characteristic length scale $L(t)$. There are a variety of equivalent definitions for this quantity. Here, we define the length scale as the reciprocal of the first moment of the scalarized structure factor, i.e., $L(t)=\langle k\rangle^{-1}$, where

$$\langle k\rangle=\frac{\int_0^{k_m}dk\,kS(k,t)}{\int_0^{k_m}dk\,S(k,t)}. \tag{11}$$

In Eq. (11), the upper cutoff k_m is taken to be half the magnitude of the largest wave vector lying in the Brillouin zone of the discrete lattice. We have confirmed that the structure factor has decayed sufficiently up to k_m so that the measured value of $\langle k\rangle$ is unaffected by an increase in k_m.

Figure 1(a) plots data for the scaled structure factor $S(k,t)\langle k\rangle^2$ vs the scaled wave vector $k/\langle k\rangle$ from dimensionless times 2100, 6300, and 10 500 for the three-state clock model. For purposes of comparison, we have also super-

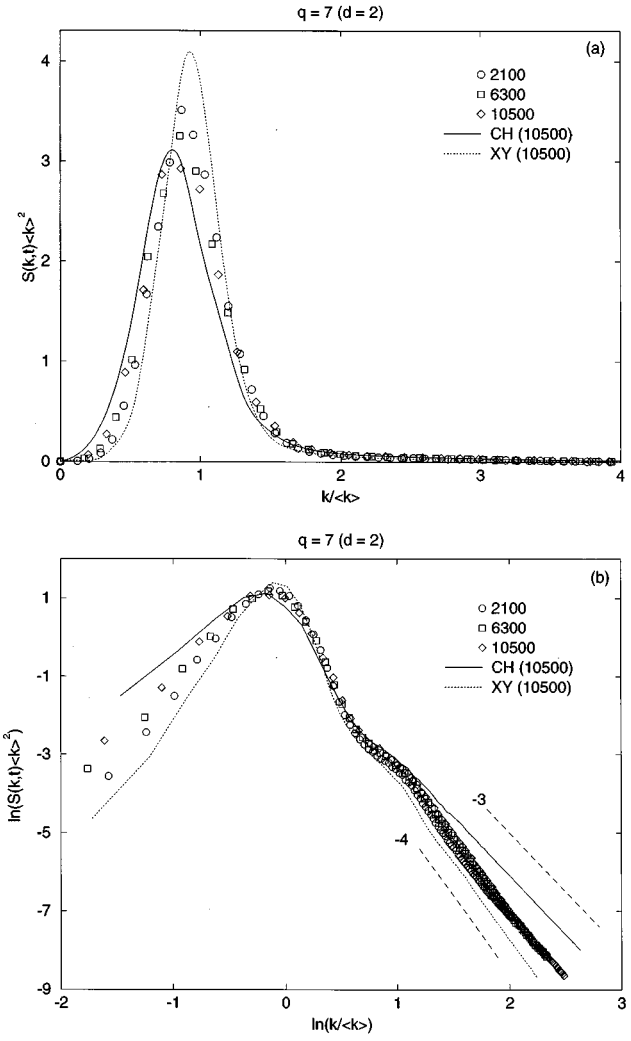

FIG. 3. (a) Analogous to Fig. 1(a), but for $q=7$. (b) Data from (a), plotted on a log-log scale.

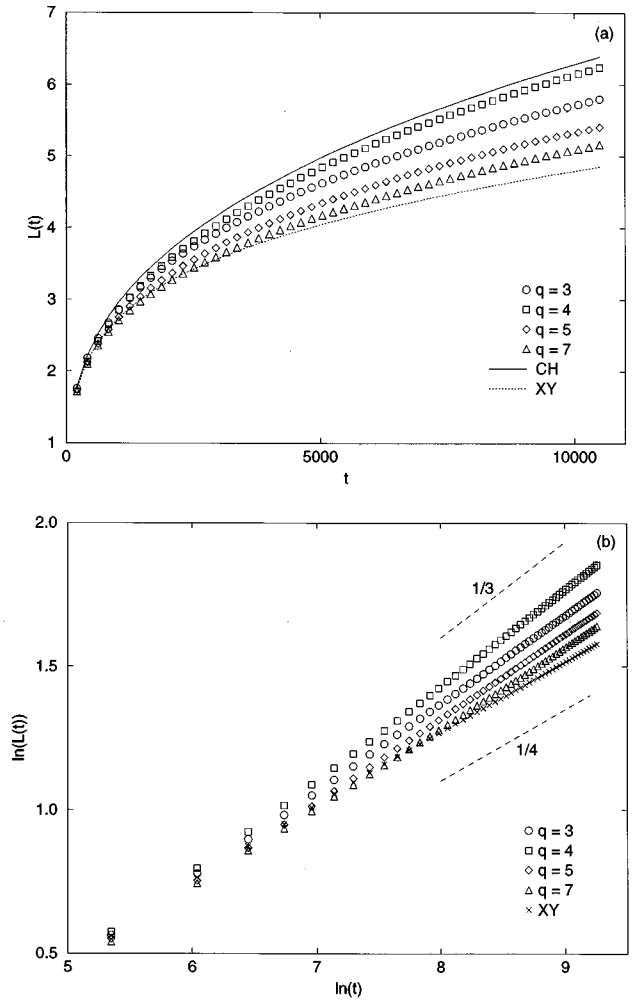

FIG. 4. (a) Characteristic length scale $L(t)$ vs t, obtained from 2D simulations of the conserved clock model. The characteristic length scale is defined as the inverse of the first moment of the scalarized structure factor. We present data for $q=3$, 4, 5, and 7; and also for the CH and XY models. (b) Data from (a), plotted on a log-log scale. We exclude the data for the CH model, for which the growth law is well understood. The dashed line with slope 1/3 refers to the Lifshitz-Slyozov growth law, which characterizes asymptotic domain growth in the CH model. The dashed line with slope 1/4 refers to the slower domain growth law [i.e., $L(t)\sim t^{1/4}$] for the conserved XY model in two dimensions [13–15].

posed the scaled structure factor for the CH model (solid line) and the XY model (dashed line). Clearly, the three-state clock model does not exhibit dynamical scaling over the entire time range considered. Rather, the scaled structure factor shows a crossover from an early-time behavior, which is intermediate between the CH and XY models, to a late-time behavior, which is reminiscent of the CH model. Figure 1(b) plots the data from Fig. 1(a) on a log-log scale so as the clarify the nature of the tail behavior. In all cases here, the structure factor data have been obtained after hardening the order parameter field, i.e., setting the absolute value of the order parameter to unity. This is done so as to clearly extract the tail behavior. The CH structure factor exhibits the usual Porod tail [$S(k)\sim k^{-(d+1)}$ for large k], whereas the XY structure factor shows the generalized Porod tail [$S(k)\sim k^{-(d+2)}$ for large k [10]]. The structure factor data

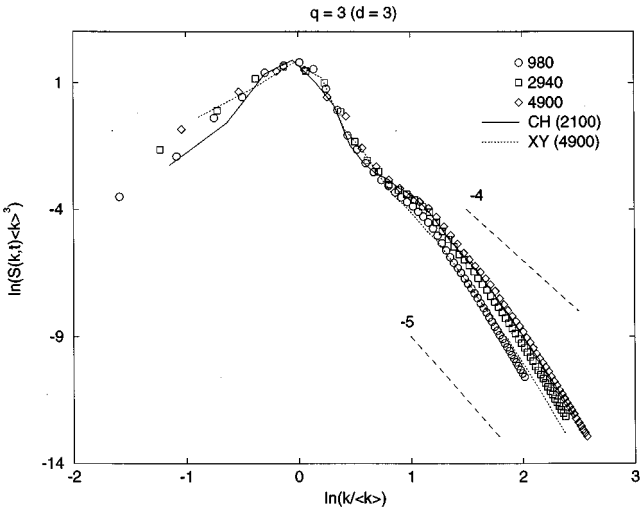

FIG. 5. Log-log plot of data for the scaled structure factor $S(k,t)\langle k\rangle^3$ vs $k/\langle k\rangle$, obtained from a 3D simulation of phase ordering dynamics in the $q=3$ clock model with a conserved order parameter. The structure factor data presented here are obtained on a 64^3 lattice as an average over 50 independent runs. For our 3D data, the order parameter field is not hardened before computing the structure factor. The data presented are from dimensionless times 980, 2940, and 4900. For reference, we also include data obtained from a similar simulation of the 3D CH model (at $t=2100$, denoted by a solid line), and the 3D XY model (at $t=4900$, denoted by a dashed line). The long-dashed lines have the same meaning as in Fig. 1(b), except they refer to the 3D versions of the Porod law and generalized Porod law [10].

for the three-state clock model follow the CH tail over a small range but deviate from it at very large values of k. This is probably a crossover effect as there is a systematic rise in the tail towards the CH tail. This is in accordance with our belief that late-stage domain growth in the clock model is driven by the annihilation of interfacial defects.

Figures 2(a) and 2(b) are analogous to Figs. 1(a) and 1(b), but for the case $q=4$. The four-state clock model is somewhat unusual in that it is isomorphic to a pair of noninteracting Ising models [17]. As a matter of fact, the analytic form

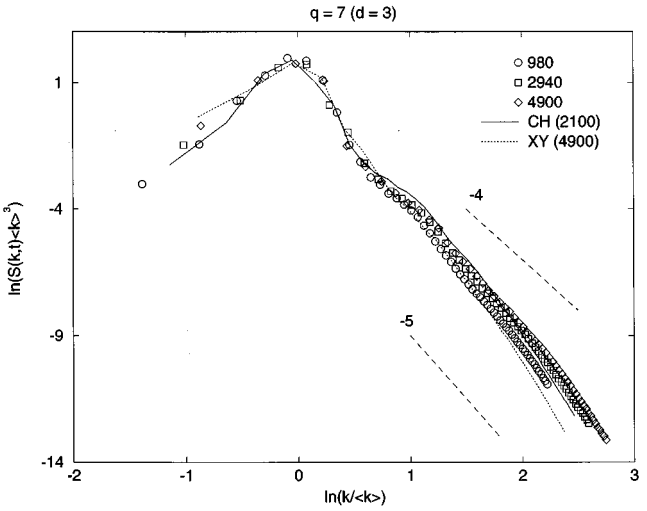

FIG. 6. Analogous to Fig. 5, but for $q=7$.

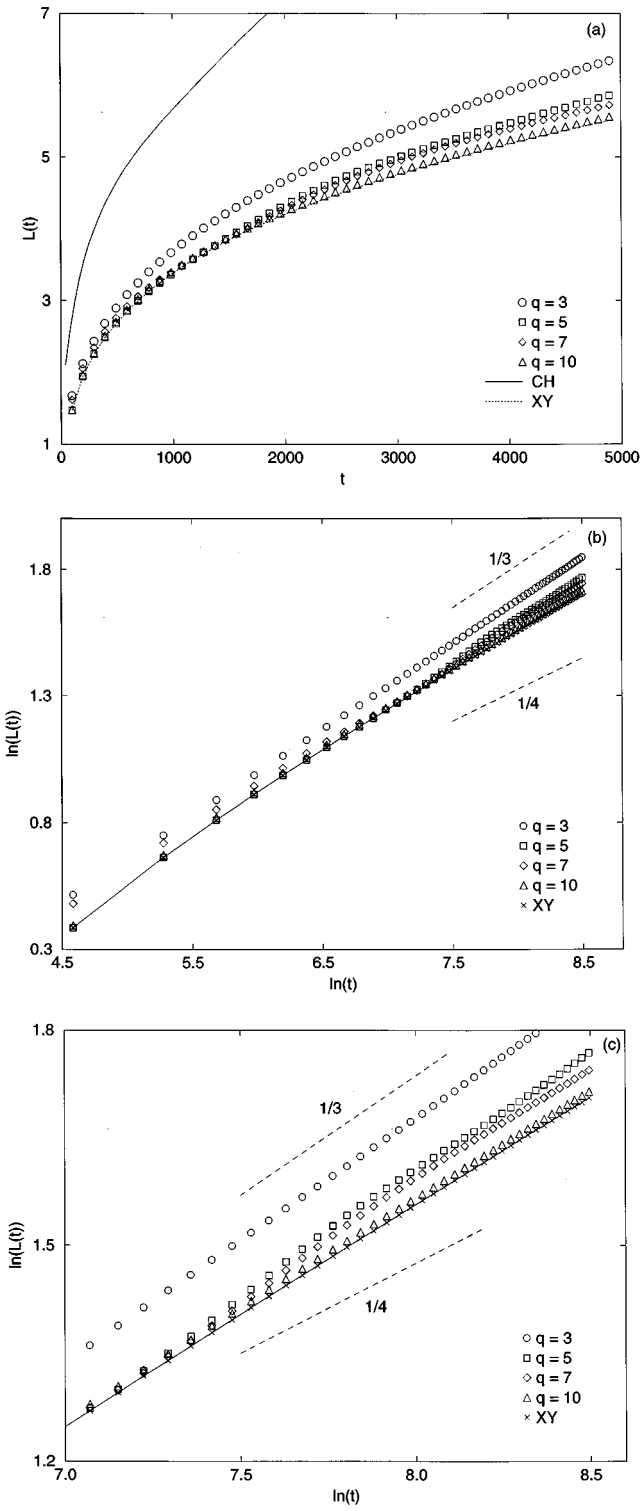

FIG. 7. (a) Characteristic length scale $L(t)$ vs t, obtained from 3D simulations of the conserved clock model. We present data for $q=3$, 5, 7, and 10; and also for the CH and XY models. (b) Data from (a), plotted on a log-log scale. Again, we have excluded the data from the CH model. The dashed lines have the same meaning as in Fig. 4(b). Notice that domain growth in the 3D conserved XY model is characterized by the law $L(t)\sim(t\ln t)^{1/4}$ (denoted by a solid line superposed on the data for the XY model) [14,15] rather than $L(t)\sim t^{1/4}$, as in the 2D case. (c) Late-time window of (b), so as to enable the reader to clearly distinguish between the different data sets.

of the scaled structure factor for the NCOP four-state clock model is identical to that for the Ising model [8]. This equivalence does not appear to have strong consequences for the form of the scaled structure factor in the COP case, though it does reflect in the growth law, as we will see shortly. As far as the scaled structure factor is concerned, the broad features are the same as those discussed for $q=3$. For completeness, we also show the scaled structure factors for the seven-state clock model in Figs. 3(a) and 3(b).

Figure 4(a) plots the characteristic length scale $L(t)$ vs t for the cases with $q=3$, 4, 5, and 7, and the CH and XY models. It is interesting to note that the length scale for the $q=4$ case grows faster than the length scale for $q=3$. This is in contrast to the general trend that higher-q clock models exhibit slower growth as a consequence of the slower annealing of vortexlike defects. The reason for this deviation from the general trend is that the $q=4$ clock model is isomorphic to two decoupled Ising models and domain growth in this case is presumably driven only by interfacial motion. It is clear from Fig. 4(a) that the data set for $q=4$ is in close proximity to that for the CH case. Figure 4(b) plots the data from Fig. 4(a) (except those for the CH case) on a log-log scale. The length scale data for the CH and XY cases are consistent with the well-known growth laws $L(t)\sim t^{1/3}$ and $L(t)\sim t^{1/4}$ [13,14], respectively. The length scale data for the $q=4$ case also exhibit a clear Lifshitz-Slyozov behavior from the earliest times, without even a hint of the slower growth law. For other values of q, the length scale data appear to be in a crossover regime between an initially slower growth consistent with $L(t)\sim t^{1/4}$ to a faster growth regime. Presumably, the asymptotic growth behavior is the LS law but our data have not accessed this regime as yet. (Of course, it should be kept in mind that the log-log plot tends to underestimate the growth exponent somewhat, except at very late times.)

IV. NUMERICAL RESULTS FOR $d=3$

We have also simulated an Euler-discretized version of Eq. (5) on a 3D square lattice of size $N\times N\times N$, with periodic boundary conditions in all directions. The details of the simulation (e.g., parameter values, initial conditions, quantities calculated, etc.) are the same as in the preceding section. The discretization mesh sizes for our 3D simulation were $\Delta t=0.07$ and $\Delta x=1.7$. Structure factor and length scale data are obtained for $N=64$ as an average over 50 independent runs. For the present set of results, we do not harden the order parameter field before computing the structure factor.

Figure 5 plots (on a log-log scale) data for the scaled structure factor $S(k,t)\langle k\rangle^3$ vs $k/\langle k\rangle$ from dimensionless times 980, 2940, and 4900 for the three-state clock model. Again, for purposes of comparison, we superpose data for the CH model (solid line) and the XY model (dashed line). With the passage of time, the scaled structure factor again drifts from an XY-like form to a CH-like behavior. Figure 6 shows the corresponding plot for the seven-state clock model.

Figure 7(a) plots the length scale data $L(t)$ vs t for the cases $q=3$, 5, 7, and 10; and also for the CH and XY models. The domain growth in the CH model is much faster than that for the other cases. Figure 7(b) plots data from Fig. 7(a)

(except for the CH case) on a log-log scale. The data for $q=3$ exhibit slower growth for a small initial period and then rapidly cross over to LS growth. The data for $q=5$ and 7 exhibit slow crossovers from a slower growth law (consistent with XY-like growth) to a faster growth which has not yet accessed the asymptotic LS regime. The data for $q=10$ are almost indistinguishable from those for the XY model, which is fitted very well by the functional form $L(t)\sim(t\ln t)^{1/4}$ [15] (denoted by the solid line). This unusual growth law for the 3D COP XY model is consistent with the theoretical predictions of Bray and Rutenberg [14]. Figure 7(c) is a late-time window of Fig. 7(b), which helps to clearly distinguish the various data sets.

V. SUMMARY AND CONCLUSION

In this paper we have presented comprehensive results from numerical simulations of the conserved clock model in two and three dimensions. Our dynamical model is a phenomenological one, formulated in terms of a complex order parameter [11]. It is difficult to motivate this model from microscopic considerations. Nevertheless, as far as phase ordering dynamics is concerned, it is reasonable to assume that our model is in the same dynamical universality class as the microscopic model, because it explicitly contains the correct local dynamics.

Numerical simulations of our model were performed using Euler-discretized equivalents of the continuum equations [18]. The broad picture that emerges is as follows. The dynamics of coarsening in the q-state conserved clock model is intermediate to that in the CH and conserved XY models. Thus the conserved clock model orders by the annealing of both vortices and interfaces. In the early stages, the domain growth is slower and is consistent with the growth law for the corresponding XY model. However, there is a crossover to faster growth (consistent with the LS law), which occurs at progressively later times for larger values of the ground-state degeneracy q. There are also dynamical crossovers in the scaled structure factor but these are harder to classify as we expect a q dependence of the asymptotic structure factor. In particular, we expect the data for all values of q to exhibit a Porod tail $S(k,t)\sim k^{-(d+1)}$ [8] but the amplitude of this tail diminishes at larger values of q.

It is not our thesis that the results in this paper have strong experimental relevance. Rather, the motivation for this study was to guide theorists by clarifying the nature of the dynamical crossover resulting from the presence of both vortices and interfaces in a phase ordering system.

ACKNOWLEDGMENTS

S.P. is grateful to Alan Bray for inviting him to visit Manchester, where many of the results presented in this paper were obtained. He would also like to thank Gene Mazenko for a number of useful comments.

[1] For reviews, see J. D. Gunton, M. San Miguel, and P. S. Sahni, in *Phase Transitions and Critical Phenomena*, edited by C. Domb and J. L. Lebowitz (Academic Press, New York, 1983), Vol. 8, p. 267; K. Binder, in *Materials Science and Technology, Vol. 5 : Phase Transformations of Materials*, edited by R. W. Cahn, P. Haasen, and E. J. Kramer (VCH, Weinheim, 1991), p. 405; A. J. Bray, Adv. Phys. **43**, 357 (1994).

[2] K. Binder and D. Stauffer, Phys. Rev. Lett. **33**, 1006 (1974); Z. Phys. B **24**, 406 (1976).

[3] T. Ohta, D. Jasnow, and K. Kawasaki, Phys. Rev. Lett. **49**, 1223 (1982); Y. Oono and S. Puri, Mod. Phys. Lett. B **2**, 861 (1988).

[4] For recent studies, see T. Ohta and H. Nozaki, in *Space-Time Organisation in Macromolecular Fluids*, edited by F. Tanaka, M. Doi, and T. Ohta, Springer Series in Chemical Physics Vol. 51 (Springer-Verlag, Berlin, 1989); C. Yeung, Y. Oono, and A. Shinozaki, Phys. Rev. E **49**, 2693 (1994); G. F. Mazenko, *ibid.* **50**, 3485 (1994).

[5] F. Y. Wu, Rev. Mod. Phys. **54**, 235 (1982), and references therein.

[6] For numerical studies of the NCOP clock model, see K. Kaski and J. D. Gunton, Phys. Rev. B **28**, 5371 (1983); K. Kaski, M. Grant and J. D. Gunton, *ibid.* **31**, 3040 (1985); G. S. Grest and D. J. Srolovitz, *ibid.* **30**, 6535 (1984); Y. Enomoto and R. Kato, Phys. Lett. A **142**, 256 (1989); J. Phys. Condens. Matter **2**, 9215 (1990).

[7] For numerical studies of the NCOP Potts model, see P. S. Sahni, G. S. Grest, M. P. Anderson, and D. J. Srolovitz, Phys. Rev. Lett. **50**, 263 (1983); P. S. Sahni, D. J. Srolovitz, G. S. Grest, M. P. Anderson, and S. A. Safran, Phys. Rev. B **28**, 2705 (1983); G. S. Grest, D. J. Srolovitz, and M. P. Anderson, *ibid.* **38**, 4752 (1988); M. P. Anderson, G. S. Grest, and D. J. Srolovitz, Philos. Mag. B **59**, 293 (1989); S. Kumar, J. D. Gunton, and K. Kaski, Phys. Rev. B **35**, 8517 (1987); M.-H. Lau, C. Dasgupta, and O. T. Valls, *ibid.* **38**, 9024 (1988); C. Roland and M. Grant, *ibid.* **41**, 4663 (1990).

[8] For analytical studies of the NCOP clock model, see K. Kawasaki, Phys. Rev. A **31**, 3880 (1985); F. Liu and G. Mazenko, Phys. Rev. B **47**, 2866 (1993).

[9] For analytical studies of the NCOP Potts model, see C. Sire and S. N. Majumdar, Phys. Rev. Lett. **74**, 4321 (1995); Phys. Rev. E **52**, 244 (1995).

[10] A. J. Bray and S. Puri, Phys. Rev. Lett. **67**, 2670 (1991); H. Toyoki, Phys. Rev. B **45**, 1965 (1992).

[11] For numerical studies of the COP clock model, see Y. Enomoto, T. Aokage, and K. Isibasi, J. Phys. Condens. Matter **4**, L133 (1992).

[12] For numerical studies of the COP Potts model, see G. S. Grest and P. S. Sahni, Phys. Rev. B **30**, 226 (1984); C. Jeppsen and O. G. Mouritsen, *ibid.* **47**, 14724 (1993).

[13] M. Mondello and N. Goldenfeld, Phys. Rev. E **47**, 2384 (1993); M. Siegert and M. Rao, Phys. Rev. Lett. **70**, 1956 (1993).

[14] A. J. Bray and A. D. Rutenberg, Phys. Rev. E **49**, R27 (1994); A. D. Rutenberg and A. J. Bray, *ibid.* **51**, 5499 (1995).

[15] S. Puri, A. J. Bray, and F. Rojas, Phys. Rev. E **52**, 4699 (1995).

[16] T. M. Rogers, K. R. Elder, and R. C. Desai, Phys. Rev. B **37**, 9638 (1988).

[17] D. D. Betts, Can. J. Phys. **42**, 1564 (1964); M. Suzuki, Prog. Theor. Phys. **37**, 770 (1967).

[18] Because of the large mesh sizes, our discrete models are better understood as cell dynamical system (CDS) models, which are in the same dynamical universality class as the continuum equation. The underlying principles of CDS modeling are formulated in Y. Oono and S. Puri, Phys. Rev. Lett. **58**, 836 (1987); Phys. Rev. A **38**, 434 (1988); S. Puri and Y. Oono, *ibid.* **38**, 1542 (1988).